

Thermodynamic Studies of Gallium–Indium Liquid Alloys by Solid State Electrochemistry with Oxide Electrolytes

Raymond Pong and Lee F. Donaghey*

Materials and Molecular Research Division, Lawrence Berkeley Laboratory and Department of Chemical Engineering, University of California, Berkeley, California 94720

The activity of gallium in Ga–In liquid alloys was studied in a high temperature galvanic cell using calcia stabilized zirconia as an oxide electrolyte. The measured activity data for gallium in the Ga–In melts was used to calculate the interaction coefficient in the liquid alloy, which has the form $\alpha_{\text{GaIn}} = \ln \gamma_{\text{Ga}} / (1 - x_{\text{Ga}})^2 = 0.2862 + 0.0352x_{\text{Ga}} + (398.3 + 220.0x_{\text{Ga}})T^{-1}$. The derived expressions for the enthalpy and excess entropy of mixing were found to be given by $\Delta H^M = (791.4 + 218.6x_{\text{Ga}})x_{\text{Ga}}(1 - x_{\text{Ga}})$ and $\Delta S^{xs} = -(0.568 - 0.0350x_{\text{Ga}})x_{\text{Ga}}(1 - x_{\text{Ga}})$. The enthalpy of mixing reaches a maximum of 226 cal/mol at a gallium mole fraction of 0.53 at x_{Ga} . The results are compared to thermodynamic data obtained by other methods. Experimental techniques and limitations are critically reviewed.

Solid-state electrochemical methods are applicable to the study of the thermodynamic properties of Ga–In–group 5 semiconductor systems. The experimental investigations on the ternary requires that the available data on the corresponding binary systems be verified. For example, the In–Sb system has been investigated by Terpilowsky (24), Hoshino et al. (9), and Chatterji and Smith (3) using liquid and solid electrolyte techniques, and the Ga–Sb system has been explored on a limited basis by Danilin and Yatsenko (5) using a liquid electrolyte technique, adding to the earlier study of liquidus temperatures by Schottky and Bever (21).

Component activities in the Ga–In system have been reported previously by Klinedinst et al. (11) using a solid-state electrolyte technique, by Svrbely et al. (23) using liquidus determinations by resistivity measurements, and by Denny et al. (6) using cooling and melting studies and metallographic examination of quenched alloy melts.

The thermodynamic properties of In–Ga liquid alloys reported by different methods are inconsistent. In an effort to resolve these inconsistencies for Ga-rich liquid alloys, the present study was undertaken using solid-state electrochemical methods. A principal aim of the study was to evaluate the limitations of this method and to compare results with those obtained by other methods.

Theory

The study of the activity of Ga in Ga–In liquid alloys was conducted with the use of calcia-stabilized zirconia as the solid-oxide electrolyte. Use of such an oxide for the purpose of determining Gibbs energies at elevated temperatures was pioneered by Kiukkola and Wagner (10). These materials have since been used for the measurement of the Gibbs energies of formation of many oxides and the partial molar Gibbs energies of alloy components.

The interpretation of high temperature solid oxide–electrolyte emf measurements utilizes the Nernst equation. The cell used in this study is the following:



The Gibbs energy of formation of Ga_2O_3 is expressed for either half-cell as:

$$\Delta G^\circ = \mu_{\text{Ga}_2\text{O}_3} + 6\mu_{e^-} - 2\mu_{\text{Ga}} - 3\mu_{\text{O}^{2-}} \quad (1)$$

Thus the equilibration of chemical potentials gives

$$6(\mu_{e_B^-} - \mu_{e_A^-}) = 2(\mu_{\text{Ga}_B} - \mu_{\text{Ga}_A}) + 3(\mu_{\text{O}_B^{2-}} - \mu_{\text{O}_A^{2-}}) - (\mu_{\text{Ga}_2\text{O}_3B} - \mu_{\text{Ga}_2\text{O}_3A}) \quad (2)$$

The Nernst voltage and the gallium activity ratio are related to electrochemical potential differences by

$$\mu_{e_B^-} - \mu_{e_A^-} = \Delta G_e = -FE \quad (3)$$

The chemical potential difference for gallium is then

$$\mu_{\text{Ga}_B} - \mu_{\text{Ga}_A} = RT \ln \frac{a_{\text{Ga}_B}}{a_{\text{Ga}_A}} \quad (4)$$

Choosing pure Ga as the reference state gives $a_{\text{Ga}_A} = 1$. In the experimental situation given, the Ga_2O_3 remains the only solid and the Ga and Ga-alloy are liquid so that the following holds: since the electrolytes used are predominantly conductors of O^{2-} ions with transport numbers of O^{2-} better than 0.99, then O^{2-} will equilibrate between the two half-cells giving $\mu_{\text{O}_B^{2-}} = \mu_{\text{O}_A^{2-}}$. Under the above conditions, eq 2 reduces to

$$\ln a_{\text{Ga}(\text{alloy})} = -\frac{3FE}{RT} \quad (5)$$

Thus, the gallium activities can be obtained from the measured concentration cell voltages.

The solid oxide electrolytes used in this study have the nominal composition, $\text{Zr}_{0.85}\text{Ca}_{0.15}\text{O}_{1.85}$ (CSZ). Figure 1 shows the conservative and liberal lower oxygen partial pressure limits to the electrolytic domain of CSZ as derived from the data of Schmalzried (20) and Patterson (16, 17). This figure shows that the P_{O_2} in equilibrium with Ga in the temperature range of interest, 600 to 1000 °C, does not lie within the electrolytic domain of CSZ as defined by the conservative lower limit. This limit is derived from the earlier work of Schmalzried (20). The later works of Patterson, Bogren, and Rapp (16), Patterson (17), and Tretyakov and Muan (25) define domain boundaries which show that part of the Ga_2O_3 –Ga– O_2 equilibrium of interest is in the electrolytic domain of CSZ. Included in Figure 1 for comparison is the lower P_{O_2} electrolytic domain boundary of YDT as derived from the data of Tretyakov and Muan (25), Hardaway et al. (8), and Levine and Kolodney (14) and by Patterson (17). It is evident that the ionic range of YDT extends to lower oxygen partial pressures than that of CSZ.

Shown also in Figure 1 are the standard Gibbs energies of formation as a function of temperature of the various oxides of the species of interest based on a single mole of O_2 . The Gibbs energy of formation of the oxide of gallium and the oxide of indium are obtained from the data of Klinedinst and Stevenson (12, 13). The data for gaseous suboxide of gallium, $\text{Ga}_2\text{O}(\text{g})$, are derived from Seybolt (22). The data for the solid suboxide of gallium, $\text{Ga}_2\text{O}(\text{s})$, are derived from Coughlin (4). From this graph

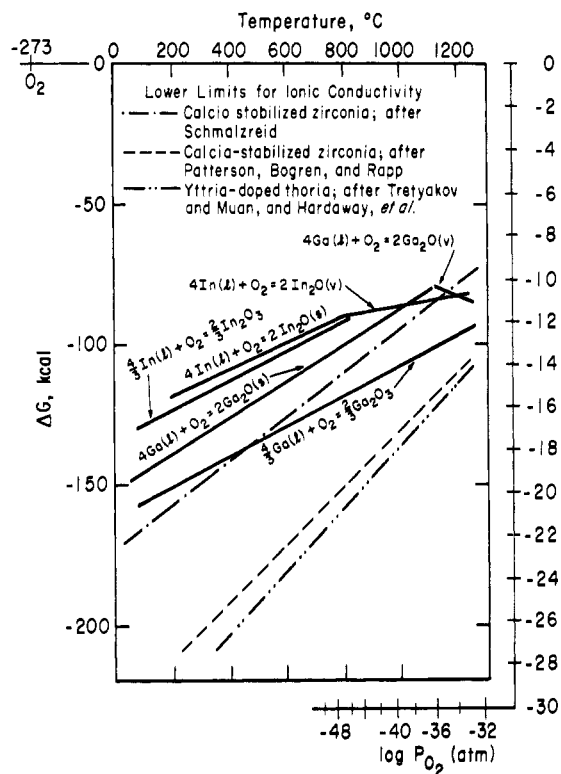


Figure 1. Gibbs energies of formation on a molar O_2 basis are compared to the lower O_2 partial pressure limits for ionic conductivity of oxide electrolytes.

it is obvious that for the temperature range of interest, the sesquioxide of gallium, Ga_2O_3 , is by far the most stable. It is estimated from the thermodynamic data that the oxide solid solution, $In_{2x}Ga_{2-2x}O_3$, should contain less than 1% In_2O_3 .

In order to study the activity of Ga in high temperature melts using a solid oxide electrolyte technique it is necessary to exclude other sources of oxygen by making measurements either under a vacuum or in a high purity inert gas atmosphere. Because of the simplicity of building and maintaining a gas tight system and purifying argon to the requisite purity, as compared to an equivalent vacuum system, measurement under an inert atmosphere was chosen. Vapor transport between the two molten electrodes was prevented by separating the atmospheres of the two electrode compartments (22).

Apparatus. An unscaled schematic of the cell is shown in Figure 2. The main cell body was an 18 in. long tube of high purity recrystallized alumina 1.5 in. o.d., 1.25 in. i.d., closed at one end (Morganite Refractories). The open end was sealed to a water-cooled stainless steel head with a buna rubber O-ring. Three ceramic tubes were passed through the head at the vertices of an equilateral triangle inscribed in a $3/8$ in. radius circle centered on the head. These ceramic tubes were sealed to the head with Viton O-rings.

A slip cast, high purity calcia-stabilized zirconia tube (Zirconia Corporation), closed at one end, served as the reference electrode compartment. Centered in this tube was a $1/8$ in. o.d. high purity alumina tube through which the high purity argon was introduced at a point near the closed bottom of the CSZ tube, as shown in Figure 2. A tungsten electrode lead was also run through this insulator to the bottom of the CSZ tube. The open top of this CSZ tube was sealed to a $1/4$ in. stainless steel Swagelok tee with a Teflon front-ferrule backed with a nylon back-ferrule. The side port from the straight run of the tee was the gas outlet for the CSZ tube venting the gas to a mercury vapor trap. A $1/8$ in. Pyrex tube at the top of the assembly was then sealed with black wax around the tungsten leads which extended completely through the assembly. The inlet gas was introduced

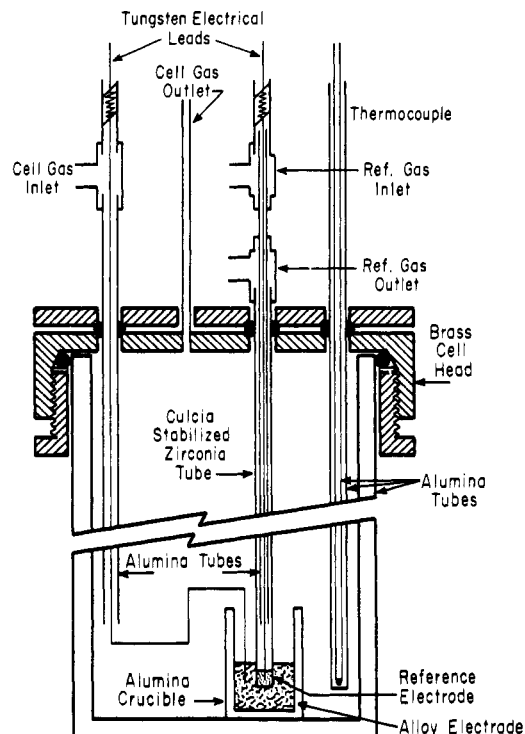


Figure 2. Schematic diagram of the experimental cell configuration for Ga-In, alloy activity studies.

through the side port of the second tee, routed by the tee configuration to the Pyrex tube and into the $1/8$ in. alumina tube. This configuration allowed a positive gas circulation in the CSZ tube.

The second ceramic tube made of high purity alumina (McDaniel Refractory Porcelain) served to transport the high-purity argon blanket gas to a point near the bottom of the main cell body. The second electrode lead was threaded through this tube. The top end of this tube was sealed to one arm of the straight run of a $1/4$ in. stainless steel swagelok tee. The other arm was sealed to a short piece of Pyrex through which the tungsten lead was threaded. The electrical lead for the sample electrode was wrapped around the tip of the CSZ tube to ensure good electrical contact with the alloy electrode, contained in a high-purity crystallized alumina crucible (Morganite Refractories), 26 mm in height and 18 mm in diameter.

The furnace was wound with Kanthal A-1 wire and powered by a proportional controller utilizing a triac gate, which controlled the temperature of the region of the sample to $0.5^\circ C$. The region of the crucible had a vertical temperature gradient of $0.2^\circ C/cm$ in the sample region. A ground shield was installed around the outer alumina tube to eliminate electrical noise created by the furnace windings.

The temperature was measured with a chromel-alumel thermocouple referenced to the melting point of ice. The measuring thermocouple was calibrated by comparison to an NBS-reference Pt + 10% Rh-Pt thermocouple over the temperature range of measurement. The thermocouple and cell emf were read with a Leeds and Northrup K-3 potentiometer. Figures 3 and 4 show the temperature control and gas manifold systems, respectively.

High purity argon gas was further purified with a Centorr gettering furnace which contained titanium turnings at $800^\circ C$. The argon gas flow rate through the purifier was maintained at less than $1\text{ ft}^3/\text{min}$ in order to improve the efficiency of the purifier. The total impurity level of the purified argon (principally CO, CO_2 , H_2O , and O_2) was estimated to be less than 0.01 ppm. Supplementary studies indicate that the oxygen activity in the purified argon was controlled by the CO- CO_2 reaction equilibrium, and that P_{O_2} was approximately 10^{-22} . Only part of the

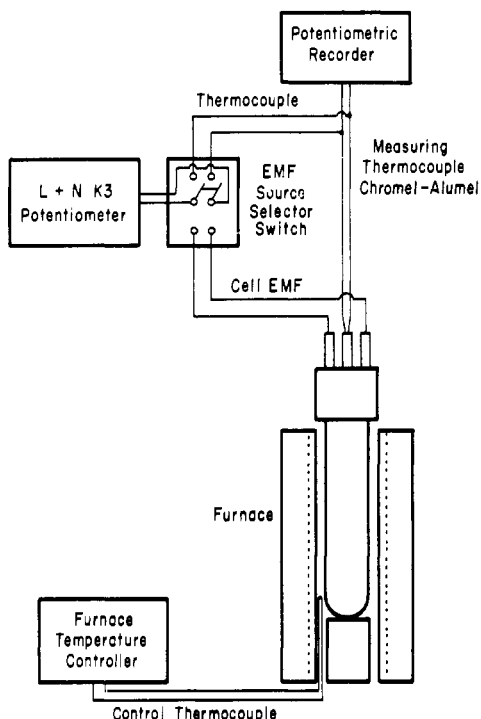


Figure 3. Temperature control and EMF measurement circuit for Ga-In alloy activity studies.

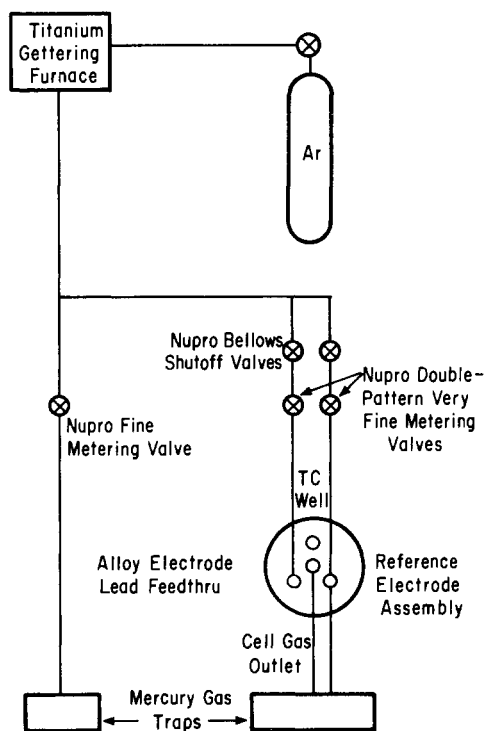


Figure 4. Gas flow system for the Ga-In alloy activity studies.

purified argon was passed through the experimental cell, with the remainder vented through mercury traps.

The cell was found to be leak-tight by a helium leak detector. This ensured a low contamination rate of the high purity argon due to permeation through seals, and to out-gassing effects.

Procedures. The reference electrode in the bottom of the CSZ tube was formed from Ca_2O_3 powder of 4-9's purity (Ventron Corp.) and Ga of 6-9's purity (Cominco American). The alloy electrode was prepared from measured amounts of Ga_2O_3 , Ga, and In of 5-9's purity (Cominco American). To secure the posi-

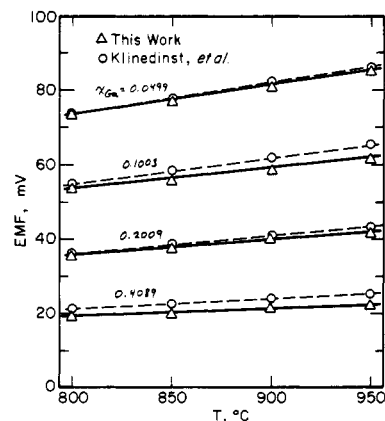


Figure 5. The experimentally measured Ga-In alloy cell emf's as a function of temperature for several alloy compositions: (—) this work, (· · ·) Klinedinst et al.

tioning of the crucible, the crucible was wired to the thermocouple tube with a short piece of tungsten wire.

At the beginning of each experiment the cell compartment was evacuated, filled with purified argon, and then purged for 2 h. Following the purge period an argon flow rate of $0.15 \text{ cm}^3/\text{s}$ was used. The cell temperature was raised to the experimental temperature at a rate of $90 \text{ }^\circ\text{C}/\text{h}$. During the heating cycle the volume expansion on heating provided a self-purging effect. During the course of the experiment the purge gas was turned off during the comparatively short periods of emf measurement to prevent any forced convection effects on cell emf measurement.

Results

The emf measured as a function of temperature in the Ga-In system is plotted in Figure 5 for the compositions investigated, along with the comparable measurements of the study by Klinedinst et al. (11). The measured cell emf was found to be highly stable with time at each temperature. In polarization experiments, the cell emf returned to a constant value following the passage of a current pulse through the cell. Thus, the oxygen activity in the reference electrode appears to be in the ionic conduction range of the solid electrolyte. Measurements below $800 \text{ }^\circ\text{C}$ required excessive equilibration times owing to flow ionic mobility of the electrolyte, while evaporation losses from the alloy electrode were excessive above $950 \text{ }^\circ\text{C}$.

Activity coefficients were calculated from the emf data which is summarized in Table I. The interaction parameter for gallium in the alloy was also calculated from the defining relation,

$$\alpha_{\text{GaIn}} = (\ln \gamma_{\text{Ga}})/(1 - x_{\text{Ga}})^2 \quad (6)$$

The interaction parameter can be expected to have the form (6, 10, 11, 23),

$$\alpha_{\text{GaIn}} = a + bx_{\text{Ga}} + c/T + dx_{\text{Ga}}/T \quad (7)$$

A least-squares fit on the data obtained from the emf measurements produced the following expression for α_{GaIn} :

$$\alpha_{\text{GaIn}} = 0.2862 + 0.0352x_{\text{Ga}} + 398.3/T + 220.0x_{\text{Ga}}/T \quad (8)$$

The rms deviation of data from this equation is ± 0.016 for the range $0.05 < x_{\text{Ga}} < 0.40$, as shown in Figure 6.

The activities of Ga at $1223 \text{ }^\circ\text{K}$ are presented graphically in Figure 7 along with the activities predicted by eq 8 and compared to the data of Klinedinst et al. (11). Using the Gibbs-Duhem equation and assuming eq 8 to apply over the composition range $0 \leq x_{\text{Ga}} \leq 1$, we obtained the activities of In which are also presented in Table I.

By using eq 8 and fundamental thermodynamic identities, the

Table I. Experimental Emf Measurements

x_{Ga}	T (°K)	Emf (mV)	a_{Ga}	a_{In}
0.0499	1073.8 ^a	73.816 ^b	0.0913	0.9514
	1123.2	77.322	0.0910	0.9514
	1174.8	81.532	0.0893	0.9513
	1224.5	85.880	0.0870	0.9513
0.1003	1073.4	53.898	0.1741	0.9048
	1124.4	56.537	0.1737	0.9047
	1174.0	59.495	0.1713	0.9046
	1223.9	62.335	0.1698	0.9045
0.2009	1073.7	35.941	0.3118	0.8182
	1124.2	38.129	0.3070	0.8177
	1174.5	40.316	0.3027	0.8173
	1224.0	42.325	0.3000	0.8169
0.4089	1073.9	19.357	0.5339	0.6573
	1124.2	20.509	0.5299	0.6556
	1174.3	21.629	0.5266	0.6540
	1224.4	22.729	0.5240	0.6526

^a The temperature accuracy is ± 0.3 °C. ^b The emf accuracy is ± 0.04 mV.

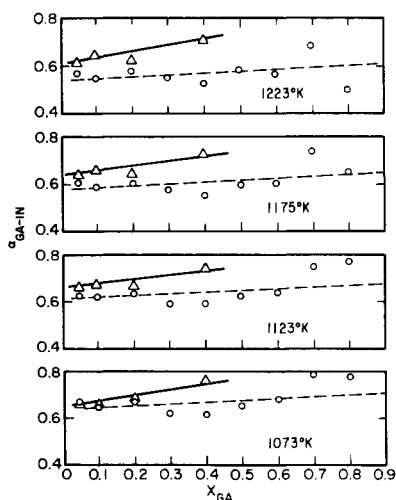


Figure 6. The $\alpha_{\text{Ga-In}}$ interaction parameters calculated from the emf data of this work (Δ) and of Klinedinst et al. (\circ) for several temperatures.

following equations for $\Delta \bar{H}_{\text{Ga}}$ and $\Delta \bar{S}_{\text{Ga}}^{\text{xs}}$ were derived from the data of this work:

$$\Delta \bar{H}_{\text{Ga}} = (791.4 + 437.1x_{\text{Ga}})(1 - x_{\text{Ga}})^2 \text{ cal/(g atom)} \quad (9)$$

$$\Delta \bar{S}_{\text{Ga}}^{\text{xs}} = -(0.5687 + 0.0699x_{\text{Ga}})(1 - x_{\text{Ga}})^2 \text{ cal/(g atom K)} \quad (10)$$

By extrapolating eq 9 and 10 over the composition range $0 \leq x_{\text{Ga}} \leq 1$, the following equations are derived, again with the aid of the Gibbs–Duhem equation:

$$\Delta H^{\text{M}} = (791.4 + 218.6x_{\text{Ga}})x_{\text{Ga}}(1 - x_{\text{Ga}}) \quad (11)$$

$$\Delta S^{\text{xs}} = -(0.5687 + 0.0350x_{\text{Ga}})x_{\text{Ga}}(1 - x_{\text{Ga}}) \quad (12)$$

The composition dependence of ΔS^{xs} , ΔH^{M} , and $\Delta \bar{H}_{\text{Ga}}$ is shown in Figure 8. The integral heat of mixing has a maximum at $x_{\text{Ga}} = 0.53$ with a value of 226 cal/mol.

Discussion

The Ga–In data obtained in this study were compared to the results of previous investigations by Macur, Edwards, and Wahlbeck (15) using Knudsen effusion by Bros (7) and Bros, Castanet, and Laffitte (2) using microcalorimetry at 150 °C, by Predel and Stein using (18) microcalorimetry at 350 °C, and by Klinedinst, Rao, and Stevenson (17) using solid–electrolyte

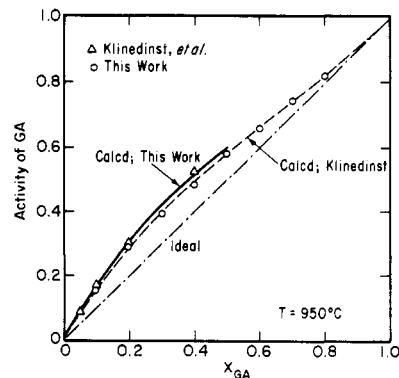


Figure 7. The activity of gallium at 950 °C as a function of the Ga–In alloy composition.

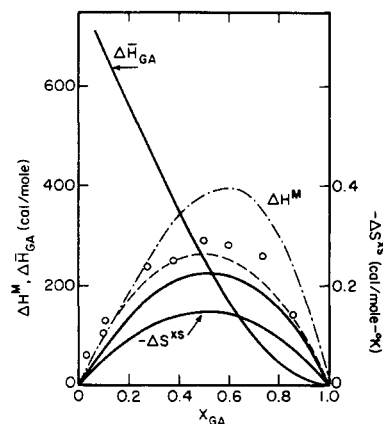


Figure 8. Enthalpy and excess entropy of mixing of Ga–In alloys as a function of gallium mole fraction: (—) this work 800–950 °C, (---) Bros 150 °C, (- - -) Klinedinst 800–950 °C, (\circ) Predel and Stein 350 °C.

techniques from 800 to 950 °C. Bros et al. conclude that the heat of mixing is symmetrical about $x_{\text{Ga}} = 0.5$, whereas the data of Predel and Stein do not confirm this symmetry, although the data of the former are not as comprehensive as those of Bros et al. The heat of mixing data derived from Gibbs energy measurements by Klinedinst et al. are also not in agreement with the conclusion of Bros et al. The scatter in the Gibbs energy data of Klinedinst et al. is sufficient to cause a reasonable error in the derived heats of mixing, which are $\sim 15\%$ larger than those obtained in the present study, as shown in eq 11.

The values of ΔH^{M} obtained by Bros et al., by Predel and Stein, and by Klinedinst et al. are not consistent with those reached by Macur et al., whose reported heat of mixing at $x_{\text{Ga}} = 0.5$ is 2200 cal/mol. The heat of mixing for $x_{\text{Ga}} = 0.5$ found by Bros et al. and Predel and Stein is 265 and 288 cal/mol, respectively, compared to a value of 212 cal/mol obtained in this study. The heat of mixing calculated from an equation, of the form of eq 7 with d set equal to 0 and fitted to the data of Klinedinst et al., gave an expression which was symmetrical about $x_{\text{Ga}} = 0.5$ with a maximum of 472 cal/mol. On the other hand, using eq 7 to fit the data of Klinedinst et al. gave a maximum value of ΔH^{M} equal to 395 cal/mol at a gallium concentration of $x_{\text{Ga}} = 0.59$, and to 381 cal/mol at $x_{\text{Ga}} = 0.5$.

The comparison of the heat of mixing data shown in Figure 8, indicates that the heat of mixing obtained in this study using high-temperature emf measurements is in agreement with the heat of mixing measurements obtained at lower temperatures by microcalorimetry. The emf results of Klinedinst et al. are significantly higher. The values for ΔH^{M} reported to Macur et al. (15) obtained by Knudsen effusion (2200 cal/mol at $x_{\text{Ga}} = 0.5$) is not at all consistent with the results of other studies.

The high temperature emf data obtained in this study and the calorimetric data of Predel and Stein suggest that the maximum heat of mixing is shifted towards the Ga rich side rather than centered at $x_{\text{Ga}} = 0.5$.

Conclusions

The thermodynamic properties of liquid gallium–indium alloys have been studied by high-temperature galvanic cell techniques using calcia-stabilized Zirconia as the solid-oxide electrolytes. The experimental method employed produced data which are quite reproducible in the temperature range from 800 to 950 °C. The derived values of the heat of mixing were found to be sensitive to the absolute errors in measurement, however. The activities of gallium in the alloys show a positive derivation from ideality. The enthalpy of mixing derived from the data of this work is consistent with values obtained by calorimetric methods.

Literature Cited

- (1) Bros, J.-P., *C.R. Acad. Sci., Ser. C*, **263**, 977 (1966).
- (2) Bros, J.-P., Castanet, R., Laffitte, M., *C.R. Acad. Sci., Ser. C*, **264**, 1804 (1967).
- (3) Chatterji, D., Smith, J. V., *J. Electrochem. Soc.*, **120**, 770 (1973).

- (4) Coughlin, J. P., Bull. 542, U.S. Bureau of Mines, U.S. Government Printing Office, Washington, D.C., 1954.
- (5) Danilin, V. N., Yatsenko, S. P., *Akad. Nauk SSSR*, **2**, 145 (1970).
- (6) Denny, J. P., Hamilton, J. H., Lewis, J. R., *J. Met.*, **39** (1952).
- (7) Etsell, T. H., Flengas, S. N., *J. Electrochem. Soc.*, **119**, 1 (1972).
- (8) Hardaway, III, J. B., Patterson, J. W., Wilder, D. R., Schieltz, J. D., *J. Am. Ceram. Soc.*, **54**, 94 (1971).
- (9) Hoshino, H., Nakamura, Y., Shimoji, M., Niwa, K., *Ber. Bunsenges.*, **69**(2), 114 (1956).
- (10) Kiukkola, K., Wagner, C., *J. Electrochem. Soc.*, **104**, 379 (1957).
- (11) Klinedinst, K. A., Rao, M. V., Stevenson, D. A., *J. Electrochem. Soc.*, **119**, 1261 (1972).
- (12) Klinedinst, K. A., Stevenson, D. A., *J. Chem. Thermodyn.*, **4**, 565 (1972).
- (13) Klinedinst, K. A., Stevenson, D. A., *J. Chem. Thermodyn.*, **5**, 21 (1973).
- (14) Levine, S. R., Kolodney, M., *J. Electrochem. Soc.*, **116**, 1420 (1969).
- (15) Macur, G. J., Edwards, R. K., Wahlbeck, P. G., *J. Phys. Chem.*, **72**, 1047 (1968).
- (16) Patterson, J. W., Bogren, C. C., Rapp, R. A., *J. Electrochem. Soc.*, **114**, 752 (1967).
- (17) Patterson, J. W., *J. Electrochem. Soc.*, **118**, 1033 (1971).
- (18) Predel, B., Stein, D. W., *J. Less-Common Met.*, **16**, 49 (1969).
- (19) Ramanarayanan, T. A., Worrell, W. L., unpublished work, 1974.
- (20) Schmalzried, H., *Z. Elektrochem.*, **66**, 572 (1962).
- (21) Schottky, W. F., Bever, B., *Acta Metall.*, **7**, 322 (1958).
- (22) Seybolt, A. U., *J. Electrochem. Soc.*, **111**, 697 (1964).
- (23) Svirbely, W. J., Sells, S. M., *J. Phys. Chem.*, **58**, 33 (1954).
- (24) Terpilowsky, J., *Arch. Hutn.*, **4**, 355 (1959).
- (25) Treyakov, J. D., Muan, M., *J. Electrochem. Soc.*, **116**, 331 (1969).

Received for review September 2, 1975. Accepted March 25, 1976.

A Review of the Osmotic Coefficients of Aqueous H₂SO₄ at 25 °C

Joseph A. Rard, Anton Habenschuss, and Frank H. Spedding*

Ames Laboratory-ERDA and Department of Chemistry, Iowa State University, Ames, Iowa 50011

Among the most widely used isopiestic standards for aqueous solutions are NaCl, KCl, CaCl₂, and H₂SO₄. The osmotic coefficient data for NaCl and KCl have recently been reviewed and appear to be known with a high degree of accuracy. The purpose of this paper is to reexamine and update the osmotic coefficient data for H₂SO₄ at 25 °C. A semiempirical equation is given which represents the osmotic coefficients of this electrolyte to within the experimental error of the data from 0.1 to 27.7 m.

This laboratory has been concerned with the measurement of the activity coefficients of aqueous rare earth chloride, perchlorate, and nitrate solutions at 25 °C by the isopiestic method. In the course of these measurements KCl, CaCl₂, and H₂SO₄ solutions have been used as isopiestic standards. We found it necessary to reexamine the standard osmotic coefficients to ensure that they were reliable enough for our calculations.

Hamer and Wu (12) have published an extensive tabulation of osmotic coefficient data for uni-univalent electrolyte solutions at 25 °C. These authors neglected to correct vapor pressure measurements for the nonideal behavior of the solvent vapor although this correction is as large as the standard deviation of their semiempirical equations for NaCl and KCl. One advantage of their data treatment is that they made the osmotic coefficient data consistent for NaCl and KCl, by use of experimental isopiestic ratios. Gibbard et al. (9) have recently reported new vapor pressure measurements for NaCl solutions and have determined least-squares equations that accurately represent both their data and other osmotic coefficient data as a function of temperature and concentration. Gibbard et al. corrected these data, when

necessary, to the presently accepted temperature scale, accepted values of the physical constants, and for the nonideal behavior of water vapor. These two reviews are in substantial agreement and the osmotic coefficients of NaCl and KCl solutions appear to be known fairly accurately.

H₂SO₄ has not received as much attention as NaCl and KCl so we decided to examine the available osmotic coefficients for this electrolyte. New data have appeared since Robinson and Stokes' review (21), and older data need to be updated with respect to temperature scales and corrected to the same values of the vapor pressure of pure water and for the nonideal behavior of water vapor. In addition, it was felt desirable to have an empirical equation to represent these osmotic coefficient data. The use of such equations would help to eliminate differences that occur when different workers use graphical interpolations of the same tabulated standard data. Such equations are available for NaCl and KCl (9, 12). No reliable equation is available which describes the H₂SO₄ data over wide concentration ranges. A future paper will deal with the osmotic coefficients of CaCl₂ solutions.

Discussion

H₂SO₄ has been used as an isopiestic standard for measurements on a number of other electrolytes. In principle each of these measurements could be used to generate H₂SO₄ osmotic coefficients, provided that accurate osmotic coefficient data are available for these other electrolytes from different measurements. It turns out, however, that NaCl and KCl are about the only salts for which accurate osmotic coefficients are available from more direct methods and for which the necessary H₂SO₄ isopiestic data exist. Because of the scarcity of accurate H₂SO₄ data at high concentrations, some of the available